

A low power ADS for transmutation studies in fast systems

Fabio Panza^{1,2,*}, Gabriele Firpo³, Guglielmo Lomonaco^{1,4}, Mikhail Osipenko¹, Giovanni Ricco^{1,2}, Marco Ripani^{1,2}, Paolo Saracco¹, and Carlo Maria Viberti³

¹ Istituto Nazionale di Fisica Nucleare – Sezione di Genova, Via Dodecaneso33, 16146 Genova, Italy

² Centro Fermi, Museo Storico della Fisica e, Centro Studi e Ricerche “Enrico Fermi”, Piazza del Viminale 1, 00184 Roma, Italy

³ Ansaldo Nucleare, Corso F.M. Perrone, 25, 16152 Genova, Italy

⁴ GeNERG DIME/TEC, University of Genova, Via. All’Opera Pia, 15/A, 16145 Genova, Italy

Received: 17 February 2017 / Received in final form: 19 June 2017 / Accepted: 10 November 2017

Abstract. In this work, we report studies on a fast low power accelerator driven system model as a possible experimental facility, focusing on its capabilities in terms of measurement of relevant integral nuclear quantities. In particular, we performed Monte Carlo simulations of minor actinides and fission products irradiation and estimated the fission rate within fission chambers in the reactor core and the reflector, in order to evaluate the transmutation rates and the measurement sensitivity. We also performed a photo-peak analysis of available experimental data from a research reactor, in order to estimate the expected sensitivity of this analysis method on the irradiation of samples in the ADS considered.

1 Introduction

The scope of this work is the study via Monte Carlo simulations (with the MCNP6 [1] and MCB [2] codes), of a fast (lead based) subcritical system to perform integral measurements. Such a system may represent an intermediate step. For example, between a zero-power accelerator driven system (ADS) like GUINEVERE [3] and future high power machines like MYRRHA [4]. In order to analyze the possible kind of measurements which can be performed at such an ADS, we have considered:

- direct fission rate evaluation, by simulating fission chambers (FC) with different fissile or fissionable isotopes depositions, photo-peak analysis of irradiated samples, as an indirect method to determine the integral fission based on the appearance of specific fission products and simulations of minor actinides (MA) irradiations in order to apply this methodology to this specific situation;
- direct method to evaluate the integral capture on U-238 based on the appearance of Np-239, this kind of approach has been used, considering the irradiation simulations of long and medium lived fission products (LLFP and MLFP), in order to estimate the transmutation rate;
- MOX time evolution by considering the appearance of some MA after a sample irradiation simulation.

2 ADS description

The geometry of the subcritical core is derived from [5], where the accelerator driver is a 70 MeV proton beam generated by a commercial cyclotron. With respect to the original studies on transmutation capabilities of the above described machine [6], we chose to double the thermal power of the system to obtain higher reaction rates. To this end, we increased the number of fuel assemblies (FAs) from 60 to 110 (increasing the lead reflector radius accordingly from 120 cm to 150 cm). We also changed the fuel from UO₂ with 20% enrichment to the Superphenix MOX composition [7], in order to consider a more standard fuel, obtaining a k_{eff} around 0.97 and a thermal power around 430 kW. The k_{source} value has been calculated using the following formula [8]:

$$P(\text{kW}) = \frac{2.9 \times 10^{-14} \cdot N_0}{\left[\frac{v \cdot k_s}{1 - k_s} \right]}, \quad (1)$$

where P in the thermal power, N_0 is the proton beam current, v is the the mean number of neutrons emitted during each fission, and the value obtained is $k_s = 0.978$. In Figure 1 the $9.6 \times 9.6 \times 150 \text{ cm}^3$ FA composed by the 0.357 cm radius and 87 cm length 81 MOX fuel pins (purple), clad by 0.07 cm steel (pink) is reported, with the helium cooling system, provided by 0.125 cm radius pipes (white), with 0.05 cm thick steel cladding (pink). The fuel pins are embedded in a solid lead matrix and the assembly is completely surrounded by a 0.2 cm steel

* e-mail: Fabio.Panza@ge.infn.it

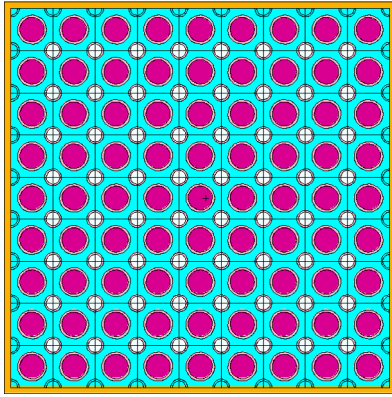


Fig. 1. FAs horizontal (xy plan) section with the fuel pins (purple) embedded in a solid lead matrix (light blue), helium pipes (white), steel claddings (pink) and steel containment (yellow).

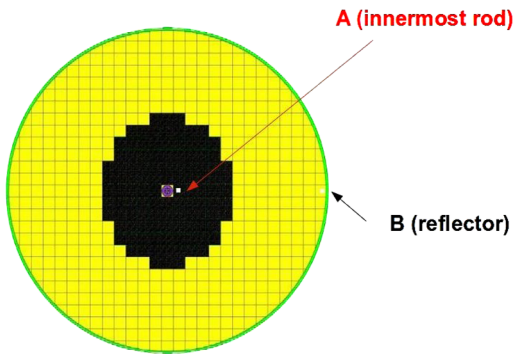


Fig. 2. 110 FAs configuration plot in xy plane with the irradiation positions: Position A is close to the source and B is located at the reflector periphery. Beryllium target (purple), reactor core (black), lead reflector (yellow), stainless steel vessel (green) are shown in the picture.

containment (yellow). The reactor core has a radius of about 80 cm, the total radius of the steel cylindrical vessel is 150 cm and the height is 150 cm, as shown in Figure 2.

All the MCNP simulations, reported here, have been performed using a measured source spectrum obtained in a dedicated experiment [9]. We assumed a proton beam with 1 mA current, corresponding approximately to a total rate of neutron production from the beryllium target of 7.6×10^{14} n/s. In Figure 1, the configuration and the selected irradiation positions A and B, namely close to the source (A) and in the lead reflector (B), are shown in the xy plane.

The neutron flux energy spectrum (the neutron flux for each energy bin or group, i.e. n/cm²/s/MeV multiplied by the bin width) in the two positions, close to the source (A) and in the lead reflector periphery (B), is plotted in Figure 3. It is evident that the spectrum in the position A presents faster characteristics with respect to the spectrum in position B; moreover, the integral flux value (the sum of the fluxes over all bins) in position A is about 35 times greater than the corresponding integral flux in the position B, as shown in Table 1.

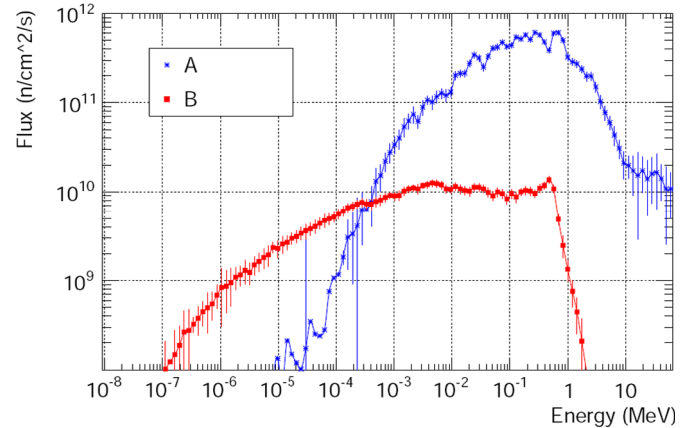


Fig. 3. Neutron flux energy spectrum (the neutron flux for each energy bin or group, i.e. n/cm²/s/MeV multiplied by the bin width) in the two positions near the source (A) and in the reflector (B).

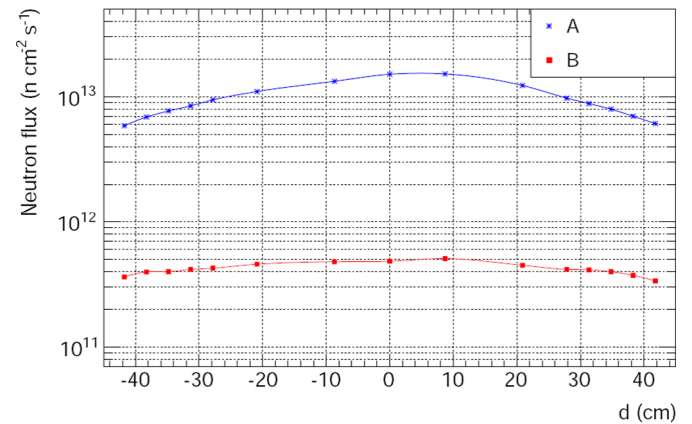


Fig. 4. Axial flux distributions in the two positions: close the source (A) and in the lead reflector (B): 0 represents the core mid-plane (error bars are smaller than the points in the plot).

The integral flux as a function of the distance d from the core mid-plane along the vertical axis (axial flux distribution), both for A and B positions, is shown in Figure 4, where it is possible to observe, as expected, that the higher flux intensity can be obtained in the axial mid-plane which represents the ideal position to perform irradiations.

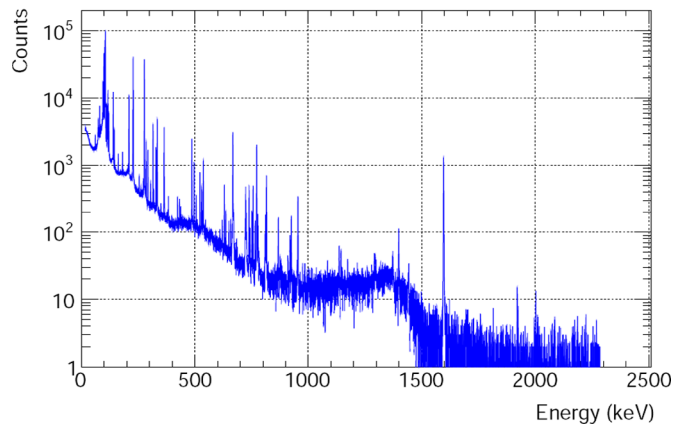
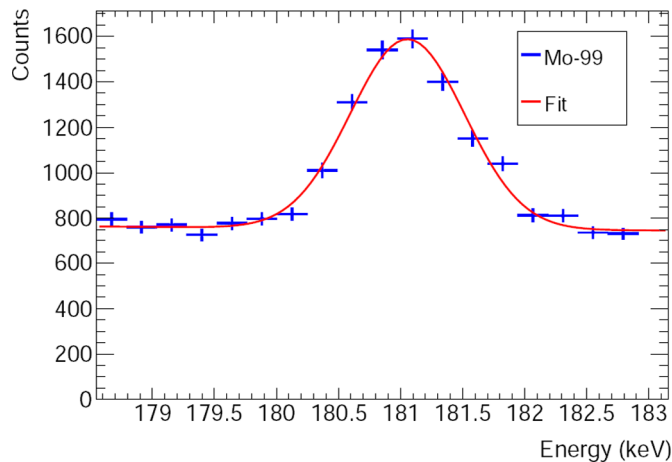
3 Fission measurements

In this section different kinds of direct and indirect fission measurements and simulations have been presented, in order to show how this system can be considered as a flexible machine for research and training purposes.

A direct evaluation of the fission rate achievable in fission chambers with different depositions (U-235, U-238, Np-237, Pu-239, Pu-241, Am-241), for each of them assuming a typical mass $m = 10 \mu\text{g}$ and assuming 100% detection efficiency has been performed. In the simulation the FC were placed in either of the two above mentioned positions (A and B in Fig. 2), in the core and in the lead reflector respectively. The results are reported in Table 2.

Table 1. Neutron fluxes in the 110 FAs configuration for the two considered positions (errors are statistical).

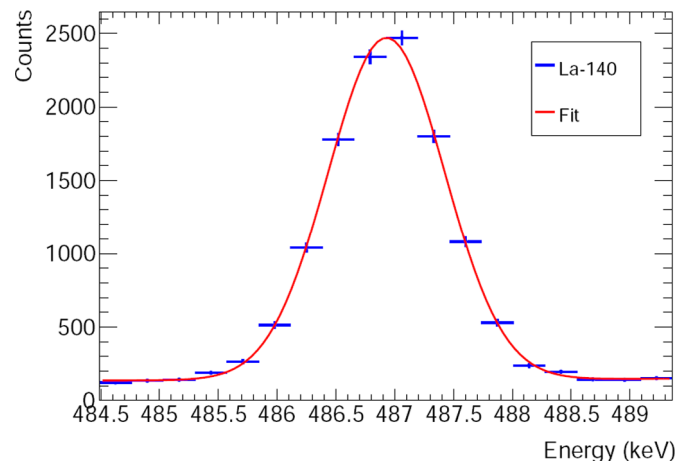
Position	Integral flux (n/cm ² /s)
A	$(1.53 \pm 0.01) \times 10^{13}$
B	$(4.82 \pm 0.01) \times 10^{11}$

**Fig. 5.** Gamma spectrum measured from a natural Uranium pellet irradiated for 6 h at 250 W in the central channel of the TRIGA MARK II facility, a thermal research reactor of the LENA laboratory (University of Pavia).**Fig. 7.** The 181.09 keV photo-peak of Mo-99, along with the ROOT fit.

These simulations give us an idea of the integral measurements of fission rates of U-235, U-238, Np-237, Pu-239, Pu-241 and Am-241 in two different reactor positions, therefore with neutron fluxes that differ in both intensity and shape. In particular, with the assumed deposited mass, which appears relatively modest, the counting rates obtained are high enough that high precision measurements can be performed within a few seconds to within several minutes (e.g., in the case of U-238 in position B).

Table 2. Fission rates R for fission chambers with different depositions. A and B are the measurement positions close to the source and in the reflector, respectively (see Fig. 1).

Material	R (fiss/s) in A	R (fiss/s) in B
U-235	$(7.15 \pm 0.20) \times 10^5$	$(3.19 \pm 0.63) \times 10^5$
U-238	$(2.51 \pm 0.03) \times 10^4$	$(2.37 \pm 0.25) \times 10^1$
Np-237	$(6.80 \pm 0.08) \times 10^5$	$(1.47 \pm 0.12) \times 10^5$
Pu-239	$(9.09 \pm 0.10) \times 10^5$	$(2.45 \pm 0.12) \times 10^5$
Pu-241	$(2.01 \pm 0.21) \times 10^5$	$(1.62 \pm 0.42) \times 10^3$
Am-241	$(1.60 \pm 0.11) \times 10^5$	$(1.01 \pm 0.07) \times 10^3$

**Fig. 6.** The 487.03 keV photo-peak of La-140, along with the ROOT fit.

As part of the integral measurements offered by the proposed ADS facility, we studied a possible method to experimentally estimate the MOX fuel burn-up. We explored the possibility to exploit gamma lines from FP appearing after irradiation, because the instrumental sensitivity may be not enough for directly measuring the disappearance of the fuel isotope components.

As a practical example, we have analyzed the gamma spectrum measured from a natural Uranium pellet irradiated for 6 h at 250 W in the central channel of the TRIGA MARK II facility, a thermal research reactor of the LENA laboratory (University of Pavia).

An HPGe detector yielded the gamma spectrum that was analyzed with the Gamma Vision[®] code by ORTEC[®]. Our purpose was to evaluate the sensitivity and the systematic uncertainty of this measurement. To get a feeling of the systematic uncertainty, we compared the results of the Gamma Vision[®] code to manual fits performed by means of the ROOT analysis framework [10]. In Figure 5 we report the gamma spectrum of the natural Uranium pellet after the irradiation.

We have considered some specific fission products featuring well-isolated and easily identifiable photo-peaks (La-140 and Mo-99) in the Gamma Vision[®] program and evaluated the activity of each single peak as reported in the code user's manual [11]. To calculate the activity of each

Table 3. Comparison of the ROOT fits and the GammaVision program for the areas of the photo-peaks of all three isotopes considered.

Nuclide	Counts from ROOT	Counts from GV
La-140	10667 ± 137	10592 ± 123
Mo-99	3921 ± 129	3704 ± 145

nuclide, we corrected the number of counts N in each peak according to the formula below, using five factors that take into account the decay during the irradiation and between the end of irradiation and the startup of counting (TDC), the total counting live time (LT), the branching ratio into that particular peak (BR), the detector efficiency (ε), and the self-absorption coefficient (A_c) [11], according to the following formula

$$A = \frac{N \cdot TDC}{LT \cdot BR \cdot \varepsilon \cdot A_c}. \quad (2)$$

The obtained numbers of counts for the selected peaks are reported in Table 3.

Then, as an alternative analysis, we have considered the region around each peak and we have fitted the peak + background with a Gaussian and a linear function (an assumption for background fit), as shown in the following formula,

$$NE = a \cdot e^{-\frac{E-t^2}{2c^2}} + d \cdot E + e, \quad (3)$$

with five parameters, in order to obtain the counting rate in the signal region using the ROOT analysis package. Obviously, in order to minimize the statistical uncertainties, we have considered the most populated (but well isolated) peaks for each isotope.

The fitted photo-peaks for La-140 and Mo-99, are shown in Figures 6 and 7, respectively,

Any difference between the peak area obtained with ROOT and Gamma Vision[®] beyond statistical uncertainties would be interpreted as systematic uncertainty. However, in the particular cases considered, we found the two independent results to be statistically compatible. The comparison between the two methods is reported in Table 3.

Obviously, longer measurements would lead to smaller statistical errors, which could reveal a systematic difference between the two methods.

Once the activity has been calculated, it is possible to perform a fuel burn-up evaluation based on the appearance of the above mentioned FP. In the present example where we analyzed the data from the TRIGA, we used the ROOT package to evaluate the burn-up of the U-235 contained in

Table 4. Calculated activities using ROOT fits for the three selected photo-peaks and corresponding evaluation of the U-235 burn-up in the data from the TRIGA reactor in Pavia.

Nuclide	Activity (Bq)	U-235 Fiss. mass (g)
La-140	$(3.62 \pm 0.05) \times 10^4$	$(1.24 \pm 0.02) \times 10^{-10}$
Mo-99	$(2.75 \pm 0.08) \times 10^4$	$(1.25 \pm 0.04) \times 10^{-10}$

the natural uranium fuel, because it is more flexible and gives the possibility to isolate each single peak and to estimate the background with different shapes and functions. In the case of the ADS with MOX fuel, the method can be applied to evaluate the main U-235 and Pu-239 burn-up together (obviously Pu-239 is both created and destroyed; here we only measure the amount of Pu-239 that underwent fission). Considering the production of a specific fission product, knowing its corresponding yield in the fission process (Y_f) and its activity (A), the burn-up, or in other words the number of fissions, can be determined using the following formula:

$$n_F = \frac{A}{\lambda \cdot Y_f}, \quad (4)$$

where λ is the nuclide decay constant. In Table 4, we report the fuel burn-up evaluated from different fission fragments.

These results have been compared with the analytic formula which gave a U-235 fissioned mass of 1.26×10^{-10} g by considering an effective fission cross section of 102 b for the central channel of the TRIGA MARK II reactor [12]. The results from the analysis of the three isotopes nicely agree with each other and with the expected value from the effective fission cross section.

While we performed this analysis using a real uranium sample irradiated in a thermal reactor, our purpose is also to find a possible way to apply this methodology to a MOX fueled fast reactor.

In order to find a possible application of this method to a MOX fuel (in which the fission fragments come mainly from U-238, U-235 and Pu-239), we propose to consider three different fission product activity measurements, thereby solving a system of three equations in three variables to distinguish the contributions from the different nuclides as reported below.

See equation (5) below

where N^{FPi} represents the number of nuclides of each single selected fission product (in our case we consider three isotopes); $Y_{U235/U238/Pu239}^{FPi}$ is the production yield of each single considered fission product from U-235, U-238 and Pu-239; $N_{U235/U238/Pu239}$ is the number of U-235, U-238 and Pu-239 fissioned nuclides.

$$\left\{ \begin{array}{l} N_{FP1} = Y_{U235}^{FP1} \cdot N_{U235} + Y_{U238}^{FP1} \cdot N_{U238} + Y_{Pu239}^{FP1} \cdot N_{Pu239} \\ N_{FP2} = Y_{U235}^{FP2} \cdot N_{U235} + Y_{U238}^{FP2} \cdot N_{U238} + Y_{Pu239}^{FP2} \cdot N_{Pu239} \\ N_{FP3} = Y_{U235}^{FP3} \cdot N_{U235} + Y_{U238}^{FP3} \cdot N_{U238} + Y_{Pu239}^{FP3} \cdot N_{Pu239} \end{array} \right. N_{FPi} \quad (5)$$

Table 5. Irradiation, decay times and results for MA pellets in position A.

Nuclide	$T_{\text{irr}} = T_{\text{dec}}$ (h)	$\Delta M/M$ (%)
Np-237	0.86	7.02×10^{-6}
Am-241	0.86	5.86×10^{-6}
Cm-244	0.86	5.31×10^{-6}

Table 6. MA fission one energy group cross sections in the A and B positions.

Nuclide	σ pos. A (b)	σ pos. B (b)
Np-237	1.5	1.0
Am-241	1.3	1.2
Cm-244	1.1	0.3

As a concrete example, we report the Mo-99 activity emerging after the irradiation in the position A (see Fig. 2) of the ADS. We considered the actinides mass equal to the U-235 mass in the sample irradiated at TRIGA (2.8 mg). After an irradiation period of 0.86 h, in which we have the same number of fissions as in the case of the natural uranium irradiation, we obtain a Mo-99 activity of 1.81×10^4 Bq. The minimum detectable activity (MDA) (6) in the regions of the spectra where some MA photo-peaks will be present. The MDA at 95% confidence level is given by [11]:

$$MDA = \frac{2.71 + 4.65 \cdot \sigma_{\text{bg}}}{LT \cdot \varepsilon \cdot BR}, \quad (6)$$

where σ_{bg} is the poissonian background standard deviation; LT is the live time of the data acquisition; ε is the detector efficiency; BR is the peak branching ratio.

We obtained a Mo-99 MDA value, of 3.16×10^4 Bq (considering the different background level due to the higher MOX activity value) for a measurement of 207 s, higher than the produced Mo-99 activity. But, for example, if we consider a 2070 s counting, the MDA is reduced by a factor 3.16, its value is 1.00×10^4 Bq, lower than the Mo-99 activity values that in this case is measurable.

One of the purposes of these studies is to show how a low-power ADS can be used for integral measurements of nuclear properties relevant to future fast lead cooled research systems. Therefore, we studied the effect of specific irradiations by using the MCB code, in order to investigate the transmutation rate of selected nuclides. In particular, we simulated the irradiation of pellets of MA, Np-237, Am-241, Cm-244, and we studied the possibility to applicate a gamma analysis on the short lived nuclides emerging by fission in the case of MA, (for example Mo-99), in order to propose a possible methodology to measure low transmutation rates (like in the considered situation). The irradiations were simulated by introducing in the core a dedicated irradiation channel near the neutron source in the equatorial position, in order to have the highest flux

Table 7. MA parents, short lived daughter nuclei produced and their activities.

Parent	Fission fragment	Activity (Bq)
Np-237	Mo-99	3.08×10^4
Am-241	Mo-99	2.07×10^4
Cm-244	Mo-99	2.575×10^5

Table 8. Comparison of the ROOT fits and the Gamma Vision[®] program for the area of the photo-peak of Np-239.

Nuclide	Counts from ROOT	Counts from GV	Diff. (%)
Np-239	139551 ± 141	144535 ± 380	3.95 ± 0.01

intensity (see Fig. 2, position A). The evolution of the pellet composition was calculated by considering a time step (T_{irr}), shorter than the saturation time of the emerging nucleus considered for the gamma analysis, as reported in Table 5 (including the natural decay) in the ADS, or the same period (T_{dec}) of pure decay, then comparing the two final compositions. The difference between the mass after T_{dec} and T_{irr} (i.e., ΔM), with respect to the initial pellet mass (i.e., M) are reported in the Table 5.

As we can see from the previous tables, the contribution of the irradiation to the transmutation, obtained by subtracting the variation due to the decay, is about $10^{-5}\%$ for MA.

In Table 6, the fission cross sections averaged over the specific neutron spectrum of positions A and B of Figure 2 (one energy group cross sections) for the considered nuclides are shown.

Due to the combination of higher integral flux and concentration of the flux in the fast region, the transmutation rate for MA is 3 orders of magnitude higher in position A than in position B. We would like to remark that even if the transmutation rates of Table 5 are low, in principle, it is possible to evaluate the transmutation of MA, reported in Tables 5 and 6, by measuring the high activity of the short lived nuclides produced by neutron capture or fission, instead of directly evaluating the small activity difference of the original nuclide before and after the irradiation, which could be beyond the experimental sensitivity.

To give an idea of the possible application of this method, in Table 7 we report the activity of Mo-99 produced after Np-237, Am-241 and Cm-244 fission starting from a pellet of 2.8 mg (the same U-235 mass in the irradiated sample at TRIGA) after a time step of 0.86 h.

Therefore we can conclude that the activity of the obtained short lived nuclei are comparable or higher with respect those measured and reported in Section 5. We remark that for the MA case, we obtain a Mo-99 activity quite similar to the one shown in Table 4, measured after irradiation of a natural uranium sample in a thermal reactor (TRIGA) operating at a power level of 250 W. Even if the U-235 fission cross section is 100 time greater in a

Table 9. Irradiation, decay times and results for MLFP pellets in position A.

Nuclide	$T_{\text{irr}} = T_{\text{dec}}$ (h)	$\Delta M/M$ (%)
Sr-90	0.86	1.25×10^{-7}
Cs-137	0.86	1.55×10^{-7}

Table 10. Irradiation, decay times and results for LLFP pellets in position A.

Nuclide	$T_{\text{irr}} = T_{\text{dec}}$ (h)	$\Delta M/M$ (%)
Tc-99	0.15	2.67×10^{-7}
I-129	0.86	9.07×10^{-7}
Cs-135	0.86	6.07×10^{-7}

Table 11. MLFP capture one energy group cross sections in the A and B positions.

Nuclide	σ pos. A (mb)	σ pos. B (mb)
Sr-90	26.9	0.5
Cs-137	32.7	1.3

thermal reactor with respect to the MA ones in a fast system, the flux is approximately 500 times lower than in the apparatus considered in this paper.

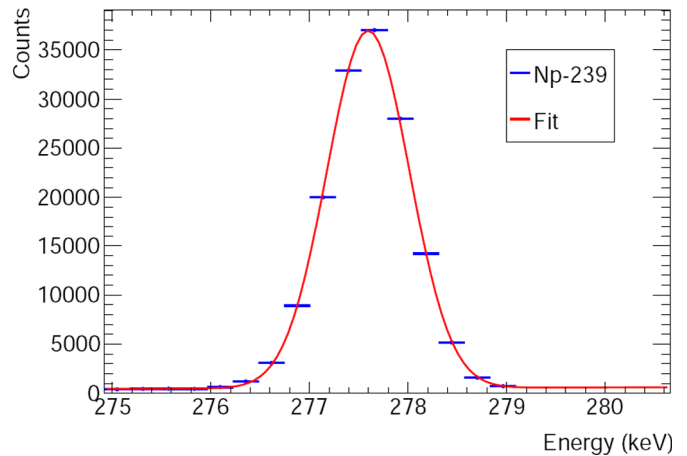
4 Capture measurements

In this section, some experimental capture measurements and simulations are described, in order to give an idea of the possible applications in fast systems.

On the same line of the experimental methodology described in Section 3, we have also fitted the Np-239 photo-peak from the TRIGA data in order to evaluate the integral capture on U-238. In this case, as shown in Table 8, the ROOT fit and the Gamma Vision[®] program turn out to be statistically incompatible, with a systematic difference of about 4%. This difference could be imputed to the fitting Gamma Vision[®] method (background estimation and peak isolation). This is obviously a guess as, being Gamma Vision[®] a commercial program, we could not investigate in detail the fitting algorithms inside the code.

For the Neptunium-239 activity, the result is $(3.72 \pm 0.01) \times 10^5$ Bq (from ROOT analysis), to be compared with the numerical calculation performed by using an effective cross section in [12], which gives 3.70×10^5 Bq. The fitted Np-239 photo-peak is shown in Figure 8.

In order to evaluate the MLFP and LLFP transmutation rate due to the capture reactions, we simulated, using MCB code, some pellets ($m = 2.8$ mg) irradiations, considering the gamma activity of the emerging short lived nuclei in a similar methodology of that described in Section 3. The evolution of the pellet composition was calculated by

**Fig. 8.** The 277.60 keV photo-peak for Np-239, along with the ROOT fit.

considering a time step (T_{irr}) shorter than the saturation time of the emerging nucleus considered for the gamma analysis, as reported in Tables 9 and 10 (including the natural decay) in the ADS, or the same period (T_{idec}) of pure decay, then comparing the two final compositions. The difference between the mass after T_{idec} and T_{irr} (i.e., ΔM), with respect to the initial pellet mass (i.e., M) are reported in the Tables 9 and 10.

As we can observe, the contribution of the irradiation to the transmutation, obtained by subtracting the variation due to the decay, is about 10^{-7} to $10^{-8}\%$ for LLFP.

The transmutation contribution for some LLFP and some MLFP is about $10^{-7}\%$, which can be easily understood if we consider their relatively small capture cross sections. In some of these cases, a softer or thermal neutron spectrum may be necessary to obtain a higher transmutation rate, and may be the subject of specific optimizations of the system. In Tables 11 and 12, the fission and capture cross sections averaged over the specific neutron spectrum of positions A and B (one energy group cross sections) for the considered nuclides are shown.

For LLFPs, the transmutation rate is the result of a balance between capture cross sections, favoring slow neutrons, from 1.4 to 2.6 times higher in position B (see Tab. 12), and absolute flux, roughly 35 times higher in position A. For this reason, we have reported in the previous tables only the results for position A. We would like to remark that even if the considered transmutation rates are low, in principle, it is possible to evaluate the transmutation of MLFP, LLFP reported in Tables 9 and 10, by measuring the high activity of the short lived nuclides produced by neutron capture or fission, instead of directly evaluating the small activity difference of the original nuclide before and after the irradiation, which could be beyond the experimental sensitivity. To give an idea of the possible application of this method, in Tables 13 and 14 we report the activities of short lived daughter nuclei produced starting from 2.8 mg pellet of medium lived and long lived parent nuclei after the irradiation period T_{irr} indicated respectively in Tables 9 and 10.

Table 12. LLFP capture one energy group cross sections in the A and B positions.

Nuclide	σ pos. A (mb)	σ pos. B (mb)
Tc-99	323.7	458.5
I-129	191.4	309.3
Cs-135	128.1	331.2

Table 13. MLFP parents, short lived daughter nuclei produced and their activities.

Parent	Daughter	Activity (Bq)
Sr-90	Sr-91	4.53×10^5
Cs-137	Cs-138	4.04×10^6

Therefore we can conclude that the activity of the obtained short lived nuclei are comparable with those measured and reported in the previous section.

5 MOX time evolution

In order to estimate the sensitivity of this method applied to the burn-up evaluation in a MOX fuel pellet placed in our reference ADS ($m = 2.8$ mg, irradiation time: 1 yr), it is useful to calculate the MDA. In this way it is possible to estimate from the MDA of some MA peaks that will be present in selected energy regions. Clearly these values are dependent from the characteristics of the background, so we will report and discuss later the results for background of similar shape but normalized to the MOX pellet activity and for the same measurement LT. The results are reported in Table 15, where we show the simulated activity for Am and Cm isotopes, along with the corresponding MDA. To calculate the MDA, it is necessary to make some assumptions about the counts from the background in a specific measurement time.

We see that Am-241, activity variations should all be detectable in a live-time of about 200 s. For the Am-243 a much longer measurement time would be needed, since the MDA is significantly larger than the activity produced in the ADS in 1 yr. Finally, the Cm-243, Cm-244 and Cm-245 are produced in a negligible and non-measurable amount.

6 Conclusions

We simulated a fast ADS based on a proton cyclotron with 70 MeV beam energy and 1 mA beam current.

The low (but non-zero) power may represent an intermediate step between zero power facilities and high power machines considered for the future. This kind of ADS, considering its characteristics and capabilities, can be considered as a safe and relatively low cost facility well suited for research, education and training purposes, aimed at both physicists and engineers.

Different fission and capture measurements both direct and indirect have been studied.

Table 14. LLFP parents, short lived daughter nuclei produced and their activities.

Parent	Daughter	Activity (Bq)
Tc-99	Tc-100	8.43×10^7
I-129	I-130	1.81×10^6
Cs-135	Cs-136	4.60×10^4

Table 15. Sensitivity of the HPGe detector to MA photo-peaks.

Nuclide	Gamma energy (keV)	ε (%)	A (Bq) after 1 yr irradiation	MDA (Bq)
Am-241	59.54	3.9	1.25×10^5	3.24×10^4
Am-243	74.76	5.4	6.31×10^1	1.91×10^4
Cm-243	276.68	9.4	7.03×10^{-1}	5.83×10^4
Cm-244	42.82	2.06	2.85×10^0	2.26×10^7
Cm-245	130.05	15.39	6.64×10^{-7}	8.45×10^4

We simulated the rate of fission chambers with fissile or fissionable isotope (U-235, U-238, Np-237, Pu-239, Pu-241, Am-241) depositions, considering two irradiation positions: close to the source and in the lead reflector periphery. Our results indicate that measurements of high precision can be performed within a few seconds to within several minutes, depending on the considered position and on the chosen deposition inside the chamber.

We performed a photo-peak analysis of an irradiated natural Uranium sample (data taken at the TRIGA reactor of Pavia), as an indirect method to determine the integral fission based on the appearance of specific FP. The analysis has been performed by evaluating the activity of the appeared fission product photo-peaks for La-140, Mo-99 and to determine the integral capture on U-238 based on the appearance of Np-239. We compared results for the peak area obtained from the Gamma Vision[®] program and from fits of the photo-peaks considered, performed with the ROOT analysis tool. The results are compatible within the statistical uncertainties except for the U-238 capture where a 4% discrepancy between the two analyses was observed. The methodology presented can be applied also to the study of the integral fission in the MOX fuel considered for the ADS described here (but also for other types of fuel), assuming the fission products to come mainly from U-235, U-238 and Pu-239, then considering the activity of at least three different isotopes and by solving a system of three equations with three unknowns (the number of fissioned nuclides). This kind of system can give us the possibility to perform integral measurements with a fast spectrum and in particular to perform a fuel burn-up analysis.

By simulating the insertion into the core (innermost rod) of various MA and FP pellets, we studied the variation of the initial isotopes, the appearance of fission products from fission of the Actinides and the transmutation by capture of the FP.

We observed that the percentage transmutation with respect to natural decay, when considering an irradiation time shorter than the saturation time in production of the daughter nuclei, is about $10^{-5}\%$ for MA, while for LLFP and MLFP is about 10^{-7} to $10^{-6}\%$. This low transmutation rate, as expected, shows that this machine cannot be considered as a transmuter (due to the low power level which makes transmutations quantitatively small even for longer irradiation times of the order of 1 yr) but only as a research facility dedicated to studies of the behavior and performance of fast sub-critical systems departing from zero power and to measurements of relevant nuclear data. We studied the possible application of an analysis based on emitted gamma from short lived isotopes produced by fission or capture. This method allows us to evaluate very low transmutation rates that would otherwise be very difficult to detect by direct observation of the amount of transmuted nuclei.

In Sections 3 and 5 a sensitivity analysis based on MDA was performed. We simulated the irradiation of a MOX and a MA sample in the considered ADS, and evaluated the MDA value in the region in which each photo-peak could be appear considering a background normalized to the higher MOX activity. The results shown as we are able to appreciate the Mo-99 and Am-241 activity variations with a reasonable counting LT.

The research leading to these results has received funding from INFN through the INFN_E strategic project, from the Centro Fermi and from the European Atomic Energy Community's (Euratom) seventh framework program FP7/2007-2011 under the project CHANDA (Grant No. 605203).

References

1. T. Goorley, "MCNP6.1.1-Beta Release Notes", LA-UR-14-24680, 2014
2. J. Cetnar et al., MCB – a continuous energy Monte Carlo Burnup code, OECD/NEA, in *Fifth international information exchange meeting, Mol* (1998)
3. A. Kochetkov et al., in *Proceedings of the second International Workshop on Technology and Components of Accelerator-driven Systems, Current progress and future plans of the FREYA project, Nantes, France, 2013* (2013)
4. H.A. Abderrahim et al., in *Proceedings of the 11th International Topical Meeting on Nuclear Applications of Accelerators (AccApp 2013), MYRRHA a flexible and fast spectrum irradiation facility, Bruges, Belgium, 2013* (2013)
5. C.M. Viberti, G. Ricco, Eur. Phys. J. Plus **129**, 66 (2014)
6. G. Lomonaco et al., Eur. Phys. J. Plus **129**, 74 (2014)
7. L. Mansani (Ansaldo Nucleare), private communication
8. H. Nifenecker, S. David, J.M. Loiseaux, O. Meplan, Nucl. Instrum. Methods **A463**, 428 (2001)
9. M. Osipenko et al., Eur. Phys. J. Plus **129**, 68 (2014)
10. <https://root.cern.ch/>
11. GammaVision[®]: gamma-ray spectrum analysis and MCA emulator for Microsoft[®] Windows[®] 7 and XP[®] professional SP3
12. A. Borio di Tigliole et al., *Preliminary TRIGA Fuel Burn-up evaluation by means Monte Carlo code and computation based on total energy released during reactor operation, PHYSOR 2012, Knoxville, Tennessee, USA, April 15–20, 2012*, on CD-ROM (American Nuclear Society, LaGrange Park, Illinois, 2012)

Cite this article as: Fabio Panza, Gabriele Firpo, Guglielmo Lomonaco, Mikhail Osipenko, Giovanni Ricco, Marco Ripani, Paolo Saracco, Carlo Maria Viberti, A low power ADS for transmutation studies in fast systems, EPJ Nuclear Sci. Technol. **3**, 36 (2017)